

Raman scattering characterization of $\text{Ga}_{1-x}\text{Al}_x\text{As}/\text{GaAs}$ heterojunctions: Epilayer and interface

P. Parayanthal and Fred H. Pollak

Physics Department, Brooklyn College of CUNY, Brooklyn, New York 11210

J. M. Woodall

IBM Thomas J. Watson Research Center, Yorktown Heights, New York 11598

(Received 12 July 1982; accepted for publication 7 September 1982)

We have used Raman spectroscopy to characterize $\text{Ga}_{1-x}\text{Al}_x\text{As}/\text{GaAs}$ heterojunctions ($x \approx 0.9$) grown by liquid phase epitaxy. The GaAs substrate had a (100) surface and the $\text{Ga}_{1-x}\text{Al}_x\text{As}$ epilayer was about 5000 Å thick. Signals were observed from both the $\text{Ga}_{1-x}\text{Al}_x\text{As}$ epilayer and the GaAs substrate at the interface. Information about the quality of the epilayer can be gained from several aspects of the spectrum including linewidths, violations of polarization selection rules (e.g., observation of symmetry forbidden TO mode), and the amplitude of the disorder-activated LA mode (DALA). These results are correlated with the properties of the substrate and growth condition. In addition the signal observed from the GaAs substrate revealed interesting features such as coupled plasmon modes and hence yielded information about band-bending and dopant diffusion at the interface.

PACS numbers: 73.40.Lq, 78.30.Jw, 81.40.Tv

Thin crystalline films and heterostructures of compound semiconductors are becoming increasingly significant for devices and device technology. The $\text{Ga}_{1-x}\text{Al}_x\text{As}/\text{GaAs}$ system is probably among the most important of the various semiconductor heterojunctions that have been fabricated during the past decade. These heterojunctions have played a key role in the development of such devices and structures as cw room-temperature injection lasers, superlattices, high efficiency solar cells, etc.^{1,2} More recently, interesting properties of the $\text{Ga}_{1-x}\text{Al}_x\text{As}/\text{GaAs}$ interface has been proposed for other uses such as Schottky barrier formation³ and passivation of the GaAs surface for metal-insulator-semiconductor (MIS) technology.⁴ In order to understand the properties of such systems it is necessary to have methods which can characterize the epilayer and interface.

In this letter we report the use of Raman spectroscopy^{5,6} to characterize both the epitaxial layer and the interface of $\text{Ga}_{1-x}\text{Al}_x\text{As}/\text{GaAs}$ ($x \approx 0.9$) heterojunctions. The structures were prepared using different modifications of the liquid phase epitaxy (LPE) method including the saturated melt mode and rapid cool modification. Signals were observed from both the epitaxial layer and the substrate at the interface. Information was obtained about (a) composition x of the $\text{Ga}_{1-x}\text{Al}_x\text{As}$ epilayer, (b) crystalline quality of the epilayer, (c) band bending at the interface, (d) carrier depletion from the GaAs substrate, and (e) carrier concentration of the GaAs substrate material.

We have studied three liquid phase epitaxial (LPE) grown samples of $n-n$ $\text{Ga}_{1-x}\text{Al}_x\text{As}/\text{GaAs}$ heterostructures as well as their GaAs substrates without the epilayer. The GaAs substrates and $\text{Ga}_{1-x}\text{Al}_x\text{As}$ epilayers were doped with Si and Te ($\approx 4 \times 10^{16}$), respectively. Two of these samples (SCL-392 and SCL-379) were prepared by the saturated melt mode. For SCL-379, the $\text{Ga}_{1-x}\text{Al}_x\text{As}$ epilayer was intentionally grown on a poor quality GaAs substrate. The third sample SCL-400 was prepared using the rapid cool

mode. The procedures and growth conditions were described in detail elsewhere.⁷ All the GaAs substrates were (100) oriented and hence so were the $\text{Ga}_{1-x}\text{Al}_x\text{As}$ epilayers. The $\text{Ga}_{1-x}\text{Al}_x\text{As}$ epilayers were of thickness ≈ 5000 Å as verified by a nondestructive nuclear profiling⁷ of the samples.

All the measurements were made from the (100) faces in the back scattering geometry using the 5145-Å laser line. In this geometry, scattering from the transverse optic (TO) mode is forbidden.^{5,6} To minimize heating the laser light was focused onto the sample with a cylindrical lens and also the samples were mounted on aluminum plates using heat conducting epoxy.

Figures 1(a), 2(a), and 3(a) display the Raman spectra of GaAs samples E-820, E-1068, and A-1319, respectively, which were used in growing the $\text{Ga}_{1-x}\text{Al}_x\text{As}$ epilayers of samples SCL-392, SCL-400, and SCL-379, respectively. Sharp structures at 269 cm^{-1} (denoted L_-) and 292 cm^{-1} (denoted LO) are seen in Figs. 1(a) and 2(a). The upper right-hand corner of both these figures exhibits a broad peak (denoted L_+). Both peaks have some sharper structure, designated $2\text{TO}(X)$ and $2\text{TO}(L)$, superimposed on them which are due to second-order two-phonon Raman scattering.⁸ Features around 165 cm^{-1} are observed in both these figures and also are due to other second-order scattering⁸ $2\text{TA}(K)$, etc. The L_- and L_+ features of Figs. 1(a) and 2(a) are the coupled plasmon-LO phonon modes^{5,6} which are observed for (100) GaAs samples with $n \geq 5 \times 10^{17} \text{ cm}^{-3}$. The fact that we observe a peak at the position of the uncoupled or "unscreened" LO mode (i.e., 292 cm^{-1}) in E-820 and E-1068 samples with such a high carrier concentration is evidence for the presence of a fully depleted space-charge layer at the surface.⁵ The penetration depth of the light is sufficiently great at 5145 Å so that Raman signals are seen from both (a) the bulk material (L_+ and L_-) and (b) the fully depleted region (where the LO phonon does not interact with the carriers), i.e., "unscreened" LO mode. The linewidth (full width

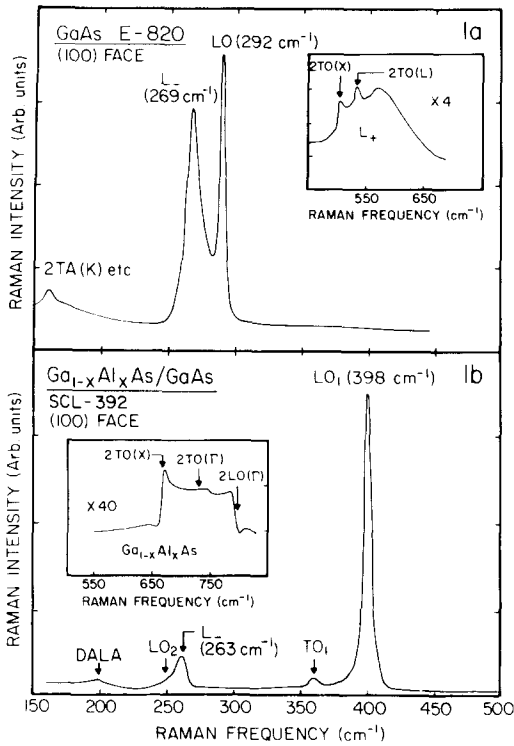


FIG. 1. (a) Raman spectrum of GaAs E-820, the substrate used in growing the Ga_{1-x}Al_xAs epilayer of sample SCL-392. The upper right-hand corner shows the coupled mode L₊. The sharper structures are due to second-order two-phonon Raman scattering. (b) Raman spectrum of Ga_{1-x}Al_xAs/GaAs sample SCL-392. The upper left-hand corner shows the Raman spectrum in the range 500–800 cm⁻¹. These Raman structures are from the Ga_{1-x}Al_xAs epilayer.

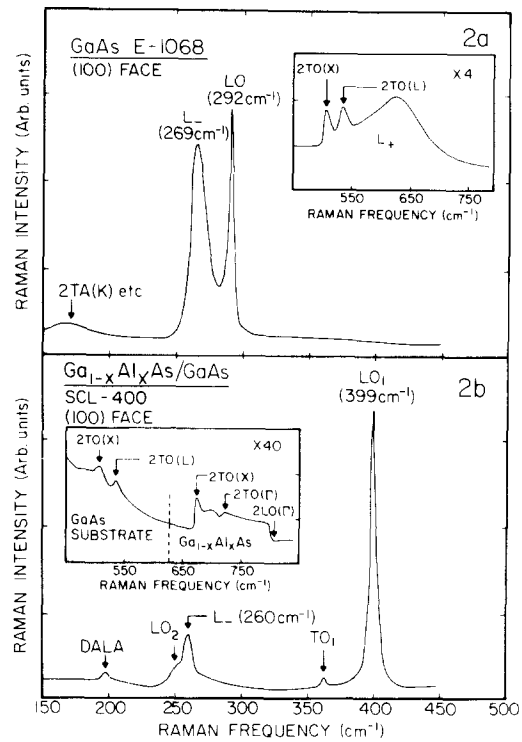


FIG. 2. (a) Raman spectrum of GaAs E-1068, the substrate used in growing the Ga_{1-x}Al_xAs epilayer of sample SCL-400. The upper right-hand corner shows the coupled mode L₊. The sharper structures are due to second-order two-phonon Raman scattering. (b) Raman spectrum of Ga_{1-x}Al_xAs/GaAs sample SCL-400. The upper left-hand corner shows the Raman spectrum in the range 500–800 cm⁻¹. The features to the left of the vertical dashed line are from the GaAs substrate and those to the right are from the Ga_{1-x}Al_xAs epilayer.

at half-maximum, corrected for instrumental resolution) for the “unscreened” LO mode is $\Gamma = 3.9 \text{ cm}^{-1}$ for sample E-820 while for sample E-1068 $\Gamma = 3.8 \text{ cm}^{-1}$. These LO phonon linewidths are comparable to other reported GaAs measurements.⁹

Figure 3(a), the Raman spectra of sample A-1319, shows no coupled modes but has a very broad LO peak ($\approx 10 \text{ cm}^{-1}$) and a clearly detectable symmetry forbidden TO mode at $\approx 267 \text{ cm}^{-1}$. The absence of the coupled modes shows that $n \leq 5 \times 10^{17} \text{ cm}^{-3}$. The linewidth of the LO peak suggests that the damage in this substrate is equivalent to the strains produced by polishing with a grit of $\approx 1.5 \mu\text{m}$ in size.⁹ The poor quality of this substrate was not confined to the surface region but extended through the bulk. We observed no significant change in the Raman spectrum even after the removal of $\approx 1000 \mu\text{m}$ of material and the subsequent preparation of the surface.

Figures 1(b) and 2(b) show the Raman spectra of Ga_{1-x}Al_xAs/GaAs samples SCL-392 and SCL-400, respectively. Signals are observed from both the Ga_{1-x}Al_xAs epilayer and the GaAs substrate at the interface. The latter is seen since the absorption coefficient for Ga_{1-x}Al_xAs ($x \approx 0.9$) at 5145 Å is small. Both of the above figures reveal two longitudinal optic (LO) modes,^{5,6,10,11} i.e., LO₁ (AlAs-like mode) at $\approx 400 \text{ cm}^{-1}$ and LO₂ (GaAs-like mode) at $\approx 250 \text{ cm}^{-1}$. The former mode has a linewidth of $\Gamma = 4.4 \text{ cm}^{-1}$ for sample SCL-400 and $\Gamma = 5.4 \text{ cm}^{-1}$ for sample

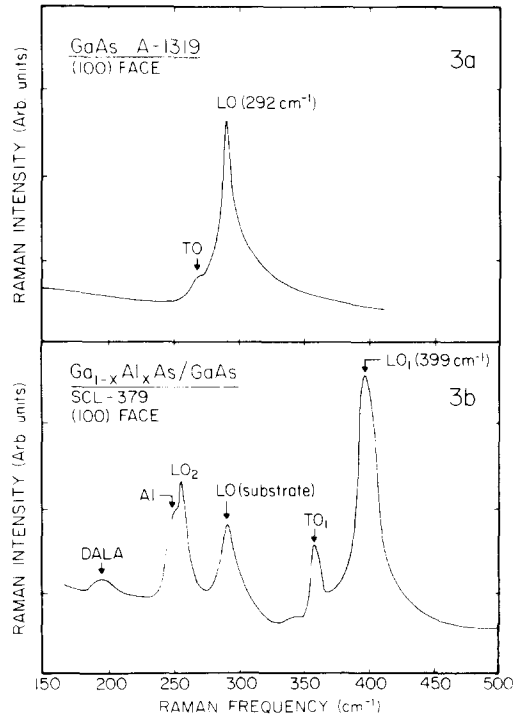


FIG. 3. (a) Raman spectrum of GaAs A-1319, the substrate used in growing Ga_{1-x}Al_xAs epilayer in SCL-379. (b) Raman spectrum of Ga_{1-x}Al_xAs/GaAs sample SCL-379.

SCL-392. Small signals from the symmetry forbidden TO_1 mode ($\approx 364 \text{ cm}^{-1}$) as well as the disorder activated longitudinal acoustic (DALA) mode ($\approx 200 \text{ cm}^{-1}$) are observed in both figures.^{6,10,11}

A signal from the GaAs substrate also was detected and is designated L_- in Figs. 1(b) and 2(b). This feature originates from the coupled modes in the GaAs at the interface. Its position is slightly down shifted in frequency from the L_- peak in the corresponding GaAs substrate spectra [see Figs. 1(a) and 2(a)]. Note also that Figs. 1(b) and 2(b) show no unscreened LO mode from the GaAs substrate.

The upper left-hand corners of Figs. 1(b) and 2(b) show the Raman spectrum between 500 cm^{-1} and 850 cm^{-1} . The structures in Fig. 2(b) to the left of the dashed vertical line, designated $2TO(X)$ and $2TO(L)$, are due to second-order two-phonon Raman scattering from the GaAs substrate. The other features between 650 cm^{-1} and 800 cm^{-1} in Figs. 1(b) and 2(b) are second order Raman scattering from the epilayer.²

Figure 3(b) displays the Raman spectrum from sample SCL-379. From the epilayer we have observed the LO_1 peak ($\Gamma \approx 13 \text{ cm}^{-1}$), symmetry-forbidden TO_1 structure as well as the LO_2 mode, DALA peak, and localized Al mode.⁶ From the GaAs substrate at the interface we have been able to detect the signal from the LO mode.

The position of the L_+ mode enables us to determine the carrier concentration^{5,6} of samples E-820 and E-1068 to be $n = (2.7 \pm 0.1) \times 10^{18} \text{ cm}^{-3}$ and $n = (3.3 \pm 0.1) \times 10^{18} \text{ cm}^{-3}$, respectively. The unscreened LO mode in such highly doped samples originates from the fully depleted space-charge region. The narrow linewidth ($\Gamma \approx 3.8 \text{ cm}^{-1}$) of this mode is evidence for the high quality of these substrates.⁹ Since sample A-1319 has $n < 5 \times 10^{17} \text{ cm}^{-3}$ only the bulk LO phonon, i.e., no coupled modes, is seen. The broad linewidth ($\Gamma \approx 10 \text{ cm}^{-1}$) of this mode and the observation of the symmetry forbidden TO mode⁵ are indications of the poor quality of A-1319.

Comparisons of Figs. 1(b) and 2(b) with Fig. 3(b) immediately reveals the difference in the crystalline quality of the various epilayers. The former samples display much narrower linewidths and, in relation to the LO_1 peak, much smaller amplitudes for the symmetry forbidden TO_1 structure and the DALA mode. SCL-400 appears to have somewhat better crystalline quality than SCL-392. The poor quality of sample SCL-379 is not surprising in view of the strained nature of the substrate material.

From the position of LO_1 and LO_2 peaks, an alloy composition of $x = 0.82 \pm 0.02$ for the epilayer of all three samples can readily be determined.^{5,6} The fact that all three samples have the same x is indicative of the controls possible in the growth procedure.

Information about the band bending of the GaAs at the interface can be deduced from absence of the "unscreened" LO phonon in Figs. 1(b) and 2(b). This observation indicates that there is no fully depleted space-charge region at the interface and hence shows the absence of band bending.

The down shift of the L_- peak of Figs. 1(b) and 2(b) in relation to its position in Figs. 1(a) and 2(a) is evidence for a

slight depletion of the carriers in the interfacial region of the substrate.

This slight depletion of carriers is probably due to a change in the n -type doping level in the GaAs surface region rather than to other effects, e.g., band bending due to interface states. A lowering of the doping concentration at the GaAs surface is expected from crystal growth considerations. First, since the GaAs substrate is doped with Si at about $3 \times 10^{18} \text{ cm}^{-3}$ and since the LPE melt is not doped with Si, the dopant is expected to outdiffuse from the GaAs substrate into the LPE melt. Secondly, the Te concentration in the melt would result in a doping of level of about 10^{17} cm^{-3} for the LPE growth of pure GaAs (it leads to a doping of $\approx 2.4 \times 10^{16}$ for $\text{Ga}_{0.15}\text{Al}_{0.85}\text{As}$).¹³ Thus, due to Si outdiffusion and low Te doping levels, the GaAs surface layer would be expected to have a lower doping concentration than the bulk. From the position of the L_- peak position the carrier concentration of the GaAs substrate, after the epilayer was grown, can be estimated. We find the carrier concentration to be $n = 1.3 \times 10^{18}$ in SCL-392 and $n = 1.2 \times 10^{18}$ in SCL-400.

In conclusion, we have made use of Raman spectroscopy for the characterization of $\text{Ga}_{1-x}\text{Al}_x\text{As}/\text{GaAs}$ heterostructures, both epilayer and interface. The alloy composition x in $\text{Ga}_{1-x}\text{Al}_x\text{As}$ was determined. We have found that the epilayer in SCL-379 has poor crystalline quality compared to SCL-400 and SCL-392. SCL-400 appears to be slightly better in crystalline quality than SCL-392. In all three samples we found that the alloy composition to be very nearly the same, suggesting that the crystal growing technique has good control over the desired composition. Information about dopant diffusion and band bending at the interface was obtained.

¹See, for example, A. G. Milnes and D. L. Feucht, *Heterojunctions and Metal-Semiconductor Junctions* (Academic, New York, 1972), and references therein.

²See, for example, H. Hovel, *Solar Cells, Semiconductor and Semimetals* (Academic, New York, 1975), Vol. II, and references therein.

³S. C. Lee and G. L. Pearson, *Solid State Electron.* **24**, 563 (1981).

⁴H. C. Casey, Jr., A. Y. Cho, D. V. Lang, E. H. Nicollian, and P. W. Foy, *J. Appl. Phys.* **50**, 3484 (1979).

⁵See, for example, G. Abstreiter, E. Bauser, A. Fisher, and K. Ploog, *Appl. Phys.* **16**, 345 (1979), and references therein.

⁶See, for example, Raphael Tsu, *Proc. Photo-Optical Instrumentations Engineers* **276**, 78 (1981), and references therein.

⁷J. S. Rosner, P. M. S. Lesser, F. H. Pollak, and J. M. Woodall, *J. Vac. Sci. Technol.* **19**, 584 (1981).

⁸R. Trommer, E. Anastassakis, and M. Cardona, in *Light Scattering in Solids*, edited by M. Balkanski, R. C. C. Leite, and S. P. S. Porto (Flammarion, Paris, 1976), p. 396.

⁹D. J. Evans and S. Ushioda, *Phys. Rev.* **9**, 1638 (1974).

¹⁰N. Saint-Ericq, R. Carles, J. B. Renucci, A. Zwick, and M. A. Renucci, *Solid State Commun.* **39**, 1137 (1981).

¹¹B. Jusserand and J. Saprial, *Phys. Rev. B* **24**, 7194 (1981).

¹²H. Mauti, P. B. Klein, R. K. Chang, R. H. Callender, and R. J. Chicotta, in *Proceedings of the Twelfth International Conference on the Physics of Semiconductors*, edited by M. H. Pilkuhn (B. G. Teubner Stuttgart), p. 509.

¹³G. L. Pearson and D. Cheung, Quarterly Progress Report for period 1 October through 31 December 1973, Solid State Electronics Laboratory, Stanford University, California.